Time-Resolved Fluorescence and ^1H NMR Studies of Tyrosine and Tyrosine Analogues: Correlation of NMR-Determined Rotamer Populations and Fluorescence Kinetics†

William R. Laws,*,‡,§ J. B. Alexander Ross,*,∥ Herman R. Wyssbrod,⊥ Joseph M. Beechem,# Ludwig Brand,# and John Clark Sutherland‡

Department of Biochemistry, Department of Physiology and Biophysics, and Center for Polypeptide and Membrane Research, Mount Sinai School of Medicine, New York, New York 10029, Biology Department, Brookhaven National Laboratory, Upton, New York 11973, and Department of Biology, The Johns Hopkins University, Baltimore, Maryland 21218

Received June 27, 1985

ABSTRACT: The time-resolved fluorescence properties of phenol and straight-chained phenol derivatives and tyrosine and simple tyrosine derivatives are reported for the pH range below neutrality. Phenol and straight-chained phenol derivatives exhibit single exponential fluorescence decay kinetics in this pH range unless they have a titratable carboxyl group. If a carboxyl group is present, the data follow a two-state, ground-state, Henderson–Hasselbalch relationship. Tyrosine and its derivatives with a free carboxyl group display complex fluorescence decay behavior as a function of pH. The complex kinetics cannot be fully explained by titration of a carboxyl group; other ground-state processes are evident, especially since tyrosine analogues with a blocked carboxyl group are also multiexponential. The fluorescence kinetics can be explained by a ground-state rotamer model. Comparison of the preexponential weighting factors (amplitudes) of the fluorescence decay constants with the ^1H NMR determined phenol side-chain rotamer populations shows that (1) tyrosine derivatives with a blocked or protonated carboxyl group have at least one rotamer exchanging more slowly than the radiative and nonradiative rates, and the fluorescence data are consistent with a slow-exchange model for all three rotamers, (2) the shortest fluorescence decay constant is associated with a rotamer where the carbonyl group can contact the phenol ring, and (3) in the tyrosine zwitterion, either rotamer interconversion is fast and an average lifetime is seen or rotamer interconversion is slow and the individual fluorescence decay constants are similar.

Time-resolved fluorescence of proteins has mainly been concerned with tryptophan. Tyrosine, by comparison, has received much less attention due to its relatively low absorptivity, low quantum yield when incorporated in polypeptide chains [see reviews by Longworth (1971, 1983)], Raman scatter interference as a consequence of the small fluorescence Stokes shift, masking of the tyrosyl emission by tryptophan, and the possibility of excited-state proton transfer with concomitant formation of tyrosinate complicating the decay kinetics (Laws & Brand, 1979) and spectral characteristics (Cornog & Adams, 1963; Longworth & Rahn, 1967). In spite of these potential problems, the photophysical properties of tyrosine should prove useful for studying proteins and polypeptides. These include the following: a short lifetime (3 ns or less), optimal for the characterization of nanosecond to subnanosecond motions in proteins; excited-state proton transfer to determine the presence of nearby acidic or basic groups; and the possibility of exciting tryptophan via resonance energy transfer to map, in favorable situations, the spatial relationship between tryptophyl and tyrosyl residues.

We were able to measure the time-resolved fluorescence of tyrosine and tyrosine analogues as a result of recent advances in data analysis and the availability of high-intensity, high-repetition-rate, ultraviolet pulsed light sources. Extraction of highly correlated decay parameters from a complex kinetic scheme has been greatly enhanced by the development of the global approach for analysis of time-resolved fluorescence data (Knutson et al., 1983; Beechem et al., 1983). The global method overdetermines certain parameters by establishing a linkage between parameters common to several data sets that are collected as a function of an independent variable such as wavelength, temperature, pH, or concentration. The linkage is established according to an assumed kinetic model. Our data were collected on a new single-photon-counting fluorometer that uses as its excitation source the vacuum ultraviolet storage ring of the National Synchrotron Light Source at Brookhaven National Laboratory. The synchrotron provides radiation consisting of short (about 500-ps full width at half-maximum) pulses of light at high frequency (52.9, 17.6, or 5.9 MHz) from the X-ray to the infrared, overcoming the experimental problems of low absorptivity, low quantum yield, short lifetime, and small Stokes shift encountered when the time-dependent fluorescence of tyrosine and related compounds is examined.

†Supported by NIH Grants HD-17542 (J.B.A.R.) and AM-10080 (H.R.W.), and in part by NIH Grants GM-11632 (L.B.) and AM-12925 and the Life Sciences Foundation, Inc. W.R.L., J.C.S., and the fluorescence spectrometer at station U9B of the National Synchrotron Light Source (NSLS) are supported by the Office of Health and Environmental Research, U.S. Department of Energy (USDOE). The NSLS is supported by the Office of Energy Research, USDOE. During part of the project, W.R.L. was supported by NIH Training Grant CA-09121. J.M.B. is supported by NIH Training Grant HD-07103. The NMR spectroscopy laboratory at Hunter College is supported by NSF Grant PGM-111745. Preliminary aspects of this work were presented at the 9th International Congress on Photobiology and 12th Annual Meeting of the American Society for Photobiology held in Philadelphia, PA, June 1984 (Laws et al., 1984), and at the 29th Annual Meeting of the Biophysical Society held in Baltimore, MD, Feb 1985 (Laws et al., 1985).

*Authors to whom correspondence should be addressed.

‡Brookhaven National Laboratory.

§Present address: Center for Polypeptide and Membrane Research, Mount Sinai School of Medicine, New York, NY 10029.

∥Department of Biochemistry, Mount Sinai School of Medicine.

⊥Department of Physiology and Biophysics and Center for Polypeptide and Membrane Research, Mount Sinai School of Medicine.

#The Johns Hopkins University.

0006-2960/86/0425-0599$01.50/0

An earlier study of time-resolved tyrosine fluorescence at one pH (Gauduchon & Wahl, 1978) reported complex decay kinetics and postulated that this behavior was due to rotameric populations of the phenol ring about the C^{α}–C^{β} bond. Rotamers having different lifetimes have also been suggested as the cause of the multiexponential decay of tryptophan systems (Donzel et al., 1974; Szabo & Rayner, 1980; Robbins et al., 1980, Ross et al., 1981). For tryptophan, direct correlation of the kinetics with independently obtained ^{1}H NMR[1] data has not been established (Szabo & Rayner, 1980; Chang et al., 1983; Petrich et al., 1983). We undertook the present study to see if a correlation exists between the decay kinetics of tyrosine and rotamer populations determined by ^{1}H NMR. The following paper in this issue (Ross et al., 1986a) reports on the fluorescence decay of tyrosine in conformationally well-characterized, small polypeptides.

Materials and Methods

Chemicals. Phenol, anisol, *p*-cresol, and 3-(*p*-hydroxyphenyl)propionic acid were purchased from Aldrich Chemical Co. (Milwaukee, WI). All other compounds were obtained from Vega Chemicals (Tucson, AZ). All compounds were used without further purification. Purity was checked by thin-layer chromatography. HPLC-grade water was from Burdick and Jackson Laboratories, Inc. (Muskegon, MI). HCl was reagent grade.

Fluorescence Spectroscopy. Steady-state spectra were obtained on an SLM 4800 fluorometer with an 8-nm bandwidth for both excitation and emission. Time-resolved data were collected on the single-photon-counting instrument at port U9B of the National Synchrotron Light Source at Brookhaven National Laboratory (Laws & Sutherland, 1986). Excitation and emission wavelengths were 284 and 302 nm, respectively, with less than 5-nm band-passes for both; scattered light was not observed under these conditions. Sample optical densities were between 0.1 and 0.2 at 284 nm. The net polarization of the excitation was measured to determine the appropriate magic angle at which to set an emission polarizer to eliminate kinetic intensity artifacts that arise from rotational motion of fluorescent molecules during the excited-state lifetime (Paoletti & LePecq, 1969; Azumi & McGlynn, 1962; Kalantar, 1968; Shinitzky, 1972). In all measurements the samples were unbuffered. The pH was adjusted with HCl and recorded in the cuvette both before and after data collection. If the pH varied by more than 0.1, the data set was disregarded and a new data set was taken. The sample temperature was maintained at 5 °C.

Fluorescence decay curves were analyzed on a VAX 11/730 computer by using a program employing a nonlinear least-squares method (Knight & Selinger, 1971; Grinvald & Steinberg, 1974), assuming that the decay was a sum of first-order processes. The fitting of the data was evaluated by the minimum reduced χ^2 value as well as by the weighted residuals between the data and the fit generated by the theoretical parameters. Decay curves were typically collected to 15 000 counts in the peak channel. We accurately recovered lifetimes for single exponential standards with reduced χ^2 values between 1.2 and 1.4. These χ^2 values were for data analyses starting at the leading edge (0.1–0.5% of the peak counts) of the instrument excitation function and continuing to 0.5% of the peak counts in the decay curve, or for about

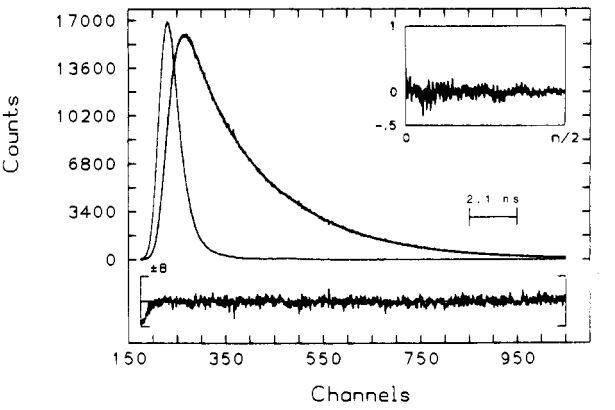

FIGURE 1: Fluorescence decay data for PPA at pH 4.71 and 5 °C analyzed for the sum of two exponentials: $\alpha_1 = 0.59$, $\tau_1 = 0.56$ ns, $\alpha_2 = 0.93$, and $\tau_2 = 3.43$ ns with $\chi^2 = 1.32$. Displayed are the instrument response function (lamp), the collected fluorescence decay curve, and the exponential parameters convolved with the lamp. The weighted residuals are shown below, while the inset contains the autocorrelation funtion of the residuals.

18 ns, whichever occurred first. The 18-ns cutoff is necessary since excitation pulses occur every 19 ns; the cutoff truncates data for samples with longer lifetimes. Even at the lower operating frequencies (17.6 or 5.9 MHz), weak excitations still occur every 19 ns due to partial population of the remaining theoretical bunches of electrons circulating in the storage ring. The partially populated bunches have different time distributions and lifetimes than the main bunch(es). Consequently, samples and standards exhibiting long-lived decays showed distortion at the beginning of the rising edge of the main excitation, as clearly shown by the weighted residuals in Figure 1. This systematic artifact was reflected by higher minimum χ^2 values.

Any systematic error is cause for concern. To determine if we could study complex kinetic systems, we measured different standards with well-documented, emission wavelength dependent, multiexponential decay behavior, such as tryptophan in its zwitterion form at neutral pH (Szabo & Rayner, 1980; Ross et al., 1981; Chang et al., 1983). Our results with these standards were in good agreement with the literature. For most compounds studied, we repeated the measurements at different times during the same stored beam and with different stored beams where the partially populated bunch characteristics varied. The time-resolved fluorescence data reported in this paper were obtained under conditions where the time constants of fluorescence standards could be recovered accurately and with a precision of at least ±50 ps.

^{1}H NMR Spectroscopy and Calculation of Rotamer Populations. Each sample, preexchanged in D_2O, was prepared by dissolving 5 mg in 1 mL of D_2O, adjusting the pD to 3 with DCl, and placing it in a Wilmad 528-PP NMR tube (5-mm o.d.). All 400-MHz ^{1}H NMR spectra were obtained at 22 °C in the pulse and Fourier transform mode on a Jeol GX-400 spectrometer located at the Department of Chemistry, Hunter College of the City University of New York. The total spectral bandwidth was 5 kHz, with a line broadening of 0.3 Hz. Transients were accumulated into 16 384 words of memory. No internal reference was required since relative chemical shifts were being determined. Spectral analysis was performed by using an iterative procedure from the Jeol software package (PLX, version 3). In this way, coupling constants were obtained with an estimated accuracy of ±0.3 Hz.

The fractional populations p_I, p_{II}, and p_{III} of rotamers I, II, and III, respectively, can be calculated from the coupling constants between vicinal H^{α} and $H^{\beta R}$ ($H^{\beta S}$) (Pople, 1958;

[1] Abbreviations: ^{1}H NMR, proton nuclear magnetic resonance; PPA, 3-(*p*-hydroxyphenyl)propionic acid; HPLC, high-performance liquid chromatography.

Table I: Fluorescence Decay Parameters of Phenol and Straight-Chained Phenol Derivatives[a]

compd	pH	α_1[b]	τ_1 (ns)	α_2[b]	τ_2 (ns)
phenol	3.25		3.72		
	4.26		3.73		
	5.16		3.74		
	6.21		3.75		
anisol	3.21		4.91		
	4.11		4.91		
	5.08		4.91		
	5.91		4.89		
p-cresol	3.20		3.36		
	4.15		3.36		
	5.12		3.36		
	6.48		3.37		
tyramine	3.26		3.62		
	4.07		3.63		
	4.98		3.64		
	6.23		3.63		
PPA[c]	2.58	0.996	0.60	0.004	3.4[d]
	3.27	0.97	0.60	0.03	3.4[d]
	3.79	0.87	0.67	0.13	3.36
	4.27	0.635	0.66	0.365	3.34
	4.53	0.47	0.64	0.53	3.46
	4.71	0.37	0.65	0.63	3.44
	4.91	0.19	0.65	0.81	3.38
	5.15	0.055	0.71	0.945	3.39
	6.27			1.0	3.46

[a] Data were obtained at 5 °C with 284- and 302-nm excitation and emission, respectively, with less than 5-nm band-passes. [b] Amplitudes were normalized to a sum of 1.0. [c] PPA stands for 3-(*p*-hydroxyphenyl)propionic acid. [d] Lifetime was held constant at this value during analysis; see text.

Pachler, 1963) by the following equations, which are adaptions of forms previously used by us (Wyssbrod et al., 1977; Fischman et al., 1978):

$$p_{\mathrm{I}} = [^3J(\mathrm{H}^{\alpha}\text{–}\mathrm{H}^{\beta R}) - {}^3J_g]/\Delta^3J$$

$$p_{\mathrm{II}} = [^3J(\mathrm{H}^{\alpha}\text{–}\mathrm{H}^{\beta S}) - {}^3J_g]/\Delta^3J$$

$$p_{\mathrm{III}} = 1 - p_{\mathrm{I}} - p_{\mathrm{II}} = [{}^3J_t + {}^3J_g - [^3J(\mathrm{H}^{\alpha}\text{–}\mathrm{H}^{\beta R}) + {}^3J(\mathrm{H}^{\alpha}\text{–}\mathrm{H}^{\beta S})]]/\Delta^3J$$

where $\Delta^3J = {}^3J_t - {}^3J_g$, and ^3J_t and ^3J_g are the nominal values of coupling constants for vicinal protons in trans and gauche conformations, respectively. In our analyses we used the values proposed by Pachler (1964) for the nominal trans and gauche couplings: $^3J_t = 13.56$ Hz and $^3J_g = 2.6$ Hz. Nonsystematic errors are estimated to be ±0.03 for p_{I} and p_{II} and ±0.05 for p_{III}.

There are two underlying assumptions in the calculation of the rotamer populations of tyrosine and its analogues. First, the *pro-R* H^{β} ($\mathrm{H}^{\beta R}$) was taken to be upfield of the *pro-S* H^{β} ($\mathrm{H}^{\beta S}$), in accordance with the stereochemical assignments for *N*-acetyl-*O*-methyltyrosine reported by Kirby & Michael (1971). Second, it was assumed that there is rotational isomerism about the C^{α}–C^{β} bond of each compound studied and that the prevalent states about this bond are the three staggered conformations (rotamers). In these rotamers the vicinally located nuclei are either trans (anti-periplanar), forming a torsion angle χ^1 of 180°, or gauche (synclinal) with an angle of ±60° (as shown in Figure 4 below). The convention recommended by the IUPAC–IUB Commission on Biochemical Nomenclature is used to express conformation in terms of torsion angle (Kendrew et al., 1970).

Results

Fluorescence Kinetics of Phenols and Straight-Chained Phenol Derivatives. Table I lists the fluorescence decay parameters between pH 2 and 7 of phenol and phenol derivatives containing unbranched alkyl chains. Phenol, anisol, *p*-cresol, and tyramine exhibit monoexponential decay kinetics with invariant lifetimes in this pH range. By contrast, 3-(*p*-hydroxyphenyl)propionic acid (PPA), which has a titratable carboxyl group, requires a sum of two exponentials to fit the data adequately. The two lifetimes are constant as a function of pH, and the preexponential terms vary in accord with the Henderson–Hasselbalch relationship:

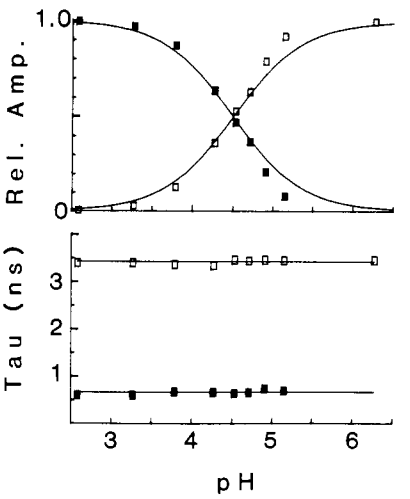

FIGURE 2: Fluorescence decay parameters of 3-(*p*-hydroxyphenyl)-propionic acid as a function of pH. The filled (open) squares indicate the association between the shorter (longer) lifetime and its amplitude. The solid lines running through the relative amplitudes express the theoretical Henderson–Hasselbalch relationship for a pK_a of 4.5. The solid lines running through the lifetimes represent their average value.

$$\log([\mathrm{A}^-]/[\mathrm{HA}]) = \mathrm{pH} - pK_a$$

as shown in Figure 2. This type of kinetic behavior is indicative of a two-state, ground-state process. In the case of PPA, protonation of the carboxyl group quenches the phenol emission from a lifetime of 3.4 ns to one of 0.6 ns. Previous steady-state investigations [see reviews by Longworth (1983) and Creed (1984)] have reported fluorescence emission quenching of tyrosine analogues when the α-carboxyl group becomes protonated. On the basis of the amplitude values (Table I and Figure 2), PPA has a pK_a of 4.5 at 5 °C, comparing favorably with the literature values of similar compounds (Greenstein & Winitz, 1961; Feitelson, 1964).

The decay data obtained for PPA as a function of pH were analyzed in three different ways. First, decay curves were analyzed singly, curve by curve, floating all four parameters of the two-component fit. The longer lifetime had a smaller value at pH 2.6 and 3.3 compared with the constant value observed at higher pH; the respective amplitude terms were larger than predicted at pH 2.6 and 3.3, suggesting a correlation between the amplitudes and the lifetimes. Second, the decay curves for these two lower pH values were reanalyzed by holding the long lifetime constant and equal to the average value at higher pH and then iterating the remaining three parameters. No change was found in "goodness of fit" criteria on performing these fixed parameter analyses for the pH 2.6 and 3.3 data sets. This result supports the notion that the long decay time and its amplitude become highly correlated when the fractional intensity contribution is small as occurs at low pH. (Dynamic quenching by H^+ has not been ruled out at this time.) The results of this analysis are the data given in Table I and Figure 2. Third, the entire pH data set was analyzed in a global manner (Knutson et al., 1983; Beechem et al., 1983), according to a model with two common lifetimes. The results of this analysis were equally satisfactory as the

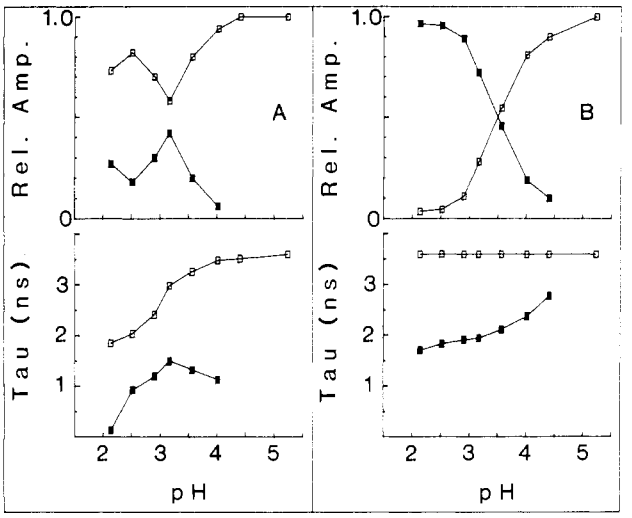

FIGURE 3: Fluorescence decay parameters of *N*-acetyltyrosine as a function of pH. (Panel A) A free-floating, two-component, curve-by-curve analysis with symbol associations as in Figure 2. (Panel B) A similar two-component analysis but with the longer decay constant held fixed at 3.4 ns. In both panels the solid lines join related data points and assume no functional model.

curve-by-curve analysis and gave lifetimes of 0.62 and 3.43 ns. The amplitude terms closely follow those shown in Figure 2.

Fluorescence of Tyrosine and Tyrosine Derivatives. The fluorescence decay kinetics, as a function of pH, are given for tyrosine and tyrosine substituted at either the α-amino or the α-carboxyl group, or both, in Table II. In all cases, the results are more complex than for any of the compounds in Table I, including PPA. Tyrosine, *O*-methyltyrosine, *N*-acetyltyrosine, and glycyltyrosine behave similarly when analyzed, curve by curve, with no restrictions on the decay parameters. Near neutral pH, where only one ionic form is in solution, these compounds can be fit by single exponentials. The statistics, however, are not as good as those obtained for single exponential standards, such as phenol. Attempts to fit two unrestricted exponentials failed. With decreasing pH, these compounds go from apparent single exponential decays to at least double exponentials (Table II). Unlike PPA, the two lifetimes and their amplitude terms show no recognizable pattern. This is shown in Figure 3A, using *N*-acetyltyrosine as an example. *N*-Acetyltyrosine was chosen since it has a more basic pK_a than tyrosine for the carboxyl group, allowing complete titration of the carboxyl group without significant H^+ quenching, which generally becomes important below pH 2 (White, 1959; Edelhoch et al., 1968; Laws & Brand, 1979).

The data of these four compounds were analyzed independently, curve by curve, in terms of a two-state, ground-state mechanism, as was done with PPA. The approach was to fit the data for two exponentials, but with the long lifetime fixed at the value from the single exponential fit at the pH where the carboxyl group is totally ionized. This analysis is shown in Figure 3B, again using *N*-acetyltyrosine to represent the behavior of all four compounds. While the amplitude terms exhibit Henderson–Hasselbalch behavior, the shorter, free-floating lifetime increases with increasing pH. Since two invariant lifetimes are required for compliance with a two-state, ground-state mechanism, the fluorescence decay of these four compounds is more complex than the decay of PPA.

Tyrosinamide, which has a blocked carboxyl group, shows no pH dependence of its decay parameters (Table II). Its fluorescence decay, however, is at least biexponential in the pH range from 2 to 6, where only the protonated amino form

Table II: Fluorescence Decay Parameters of Tyrosine and Tyrosine Derivatives[a]

compd	pH	α_1[b]	τ_1 (ns)	α_2[b]	τ_2 (ns)
tyrosine	2.06	0.19	0.96	0.81	2.08
	2.46	0.17	1.06	0.83	2.88
	2.72	0.11	1.00	0.89	3.21
	3.12	0.03	0.98	0.97	3.52
	4.53			1.0	3.73
	6.14			1.0	3.76
O-methyltyrosine	2.09	0.14	0.76	0.86	2.61
	2.44	0.15	0.72	0.85	3.45
	2.71	0.08	1.00	0.92	4.11
	3.03	0.03	1.38	0.97	4.54
	4.66			1.0	5.05
	6.20			1.0	5.06
N-acetyltyrosine	2.14	0.27	0.13	0.73	1.85
	2.52	0.18	0.93	0.82	2.04
	2.91	0.30	1.20	0.70	2.41
	3.17	0.42	1.50	0.38	2.98
	3.57	0.20	1.33	0.80	3.26
	4.02	0.06	1.13	0.94	3.48
	4.41			1.0	3.51
	5.24			1.0	3.60
glycyltyrosine	2.34	0.40	0.65	0.60	1.33
	2.95	0.41	0.78	0.59	1.51
	3.10	0.38	0.93	0.62	1.61
	3.33	0.33	0.97	0.67	1.62
	4.75			1.0	1.59
	6.46			1.0	1.65
tyrosinamide	3.36	0.33	0.46	0.67	1.87
	4.07	0.32	0.62	0.68	1.92
	5.11	0.33	0.53	0.67	1.95
	6.38	0.32	0.54	0.68	1.91
N-acetyltyrosinamide	3.23	0.14	0.83	0.86	2.18
	4.02	0.14	0.72	0.86	2.18
	5.15	0.14	0.95	0.86	2.21
	6.09	0.14	0.93	0.86	2.22
tyrosylglycine	2.10	0.44	0.45	0.56	2.19
	2.40	0.45	0.45	0.55	2.20
	2.75	0.44	0.50	0.56	2.25
	3.08	0.42	0.55	0.58	2.28
	4.14	0.44	0.72	0.56	2.31
	5.34	0.44	0.73	0.56	2.34
	6.44	0.40	0.79	0.60	2.42

[a] Data were obtained at 5 °C with 284- and 302-nm excitation and emission, respectively, with less than 5-nm band-passes. [b] Amplitudes were normalized to a sum of 1.0.

exists. Likewise, *N*-acetyltyrosinamide also exhibits multiexponential decay behavior in this pH range. These results are in agreement with those obtained by Gauduchon & Wahl (1978) for data at pH 5.5. Tyrosylglycine fluorescence decay can also be described by the sum of two exponentials with, however, a slight increase in both lifetimes with increasing pH (Table II). This pH dependence can be shown to follow protonation of the glycine carboxyl group. Steady-state results have previously shown a small quantum yield dependence on protonation of the carboxyl group of tyrosylglycine (Edelhoch et al., 1968). Since the zwitterionic form exhibits more than one exponential, the fluorescence decay of tyrosylglycine is more complex than a simple two-state, ground-state Henderson–Hasselbalch process. Additionally, the decay kinetics seen for the single chemical species in solution for tyrosinamide and *N*-acetyltyrosinamide also suggest a more complex explanation.

Excited-State Proton Transfer. Phenols are expected to undergo excited-state proton transfer, since the hydroxyl becomes a stronger acid in the excited state. Theoretical calculations predict a pK_a^* near 5 (Feitelson, 1964), and a value of 4.2 has been reported for tyrosine on the basis of steady-state measurements (Rayner et al., 1978). In contrast, the ground-state pK_a of the hydroxyl group is around 10. It has been well documented that excited-state proton transfer can

Table III: ^{1}H NMR Coupling Constants and Calculated Rotamer Populations

compd	coupling constants[a]		populations[b]		
	$^3J(H^\alpha-H^{\beta R})$	$^3J(H^\alpha-H^{\beta S})$	p_I	p_{II}	p_{III}
tyrosine	7.94	5.49	0.49	0.26	0.25
O-methyltyrosine	7.64	5.80	0.46	0.29	0.25
N-acetyltyrosine	9.16	5.15	0.60	0.24	0.16
glycyltyrosine	8.54	5.49	0.54	0.26	0.20
tyrosinamide	7.62_5	6.71	0.46	0.37	0.17
tyrosylglycine	7.32	6.71	0.43	0.38	0.19
N-acetyltyrosinamide	9.15	6.10	0.60	0.32	0.08

[a] Values given are in Hz. [b] Sum of the populations = 1.0 with errors in p_I and p_{II} of ±0.03 and in p_{III} of ±0.05.

lead to multiexponential decay behavior (Weller, 1961; Laws & Brand, 1979; Gafni et al., 1976; Gafni & Brand, 1978). The single exponential decays obtained for the compounds in Table I suggest that reversible excited-state proton transfer is not significant under the conditions studied. To ensure that excited-state proton transfer is not the cause of the multiexponential decay behavior of tyrosine and its analogues, we performed steady-state fluorescence titrations of *N*-acetyltyrosinamide in water. Constant fluorescence yield was observed between pH 3 and 8. This would not be expected if excited-state proton transfer, which can be considered as a quenching mechanism for the excited protonated species, was significant. Moreover, phenol and anisol exhibit single exponential fluorescence decay over this pH range. Since tyrosine and *O*-methyltyrosine behave similarly below pH 7 (Table II), their complex decay kinetics as a function of pH must not be a consequence of excited-state proton transfer. According to steady-state emission data, none of the compounds in Tables I and II show any evidence of phenolate emission.

^{1}H NMR of Tyrosine and Tyrosine Derivatives. Table III lists the coupling constants between the α- and β-protons of tyrosine and its derivatives. The coupling constants allow calculation, as described under Materials and Methods, of the three staggered tyrosyl rotamer populations about the C^α–C^β bond, which are diagrammed in Figure 4. Derivatization at the α-amino group results primarily in depopulation of rotamer III in favor of rotamer I, while substitution at the α-carboxyl group enhances rotamer II at the expense of rotamer III.

Discussion

Chemical and structural heterogeneity as well as excited-state reactions affects the kinetics of fluorescence decay. As a result, the fluorescence decay may be mono- or multiexponential and, in certain cases, nonexponential. Generally, two-state, excited-state proton transfer is an important process in the photophysics of hydroxylated aromatic hydrocarbons. The decay kinetics have a characteristic signature: first, the acidic and basic excited-state species have the same decay constants; second, all decay parameters vary with pH through the pK_a^*; third, the amplitudes for the basic (acidic) excited-state species are equal but opposite in magnitude when only the acidic (basic) form exists in the ground state. This kinetic system has been well studied with the hydroxylated naphthalene 2-naphthol, a stronger acid in the excited state (Laws & Brand, 1979), and with acridine, a stronger base in the excited state (Gafni & Brand, 1978). In the case of phenols in water, the constant fluorescence yield and the absence of multiexponential kinetics as a function of pH in the range of the pK_a^* (Tables I and II) suggest that they do not undergo significant reversible excited-state proton transfer. This is supported by a comparison of the excited-state rate constants,

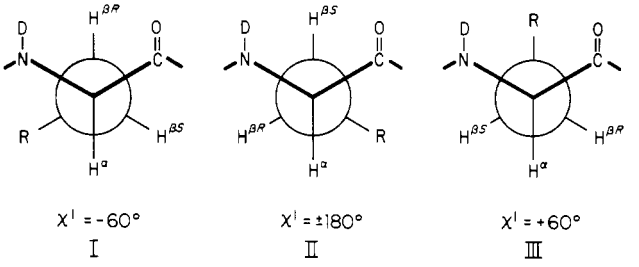

FIGURE 4: Newman projections about the C^α–C^β bond, detailing the possible positions of the phenol group in relation to the C^α substituents. The rotamer assignments I, II, and III, and the corresponding values of the torsion angle χ^1, are indicated for tyrosine or tyrosine derivatives of the L configuration. The atoms or groups attached to the backbone N and C atoms and the charged state, if any, of these latter atoms are not shown and depend on the particular compound under consideration. The atom D indicates the state of the compound in D_2O, the solvent used for the NMR studies.

and therefore pK_a^*, of 2-naphthol with the calculated and measured pK_a^* values of phenols, which indicates approximately 2 orders of magnitude slower rates of deprotonation in the excited state of phenols in water. We assume that the diffusion-controlled, bimolecular reprotonation rate is similar for 2-naphthol and phenols. Consequently, for the protonated form of phenols, excited-state proton transfer to bulk water would fail to compete kinetically with the total radiative and nonradiative decay rates. Any multiexponential decay behavior of phenols, under these conditions, cannot be ascribed to excited-state proton transfer. Moreover, proton transfer was not seen with PPA, where it is possible that the carboxyl group could act as an effective intramolecular proton transfer acceptor/donor as seen with 2-hydroxy-1-naphthaleneacetic acid (Gafni et al., 1976). However, these arguments do not preclude the possibility of excited-state proton transfer for tyrosyl residues in polypeptides if the polypeptide contains a proton acceptor group stronger than water in close proximity to the hydroxyl function. Steady-state fluorescence studies of tyrosine in the presence of high concentrations of acetate indicate that, under certain conditions, phenols indeed exhibit two-state, excited-state proton transfer (Rayner et al., 1978). In addition, evidence has been presented for excited-state tyrosinate formation in proteins (Longworth, 1981).

Excimer formation, solvent relaxation, and resonance energy transfer are other important excited-state processes that lead to complex fluorescence kinetics. These processes all exhibit characteristic decay kinetics [see review by Badea & Brand (1979)] that are not evident in our phenol and tyrosine data. Although excited-state processes cannot be entirely ruled out, the observed multiexponential behavior in the present data is not consistent with excited-state processes. The alternative explanation is ground-state heterogeneity.

Ground-state heterogeneity can arise with tyrosine and its analogues from ground-state ionization of the α-carboxyl, α-amino, and phenolic hydroxyl groups. Between pH 2 and 6 the only titratable group is the carboxyl function. Compounds with blocked carboxyl groups, or tyrosylglycine between pH 5 and 6 where only its zwitterionic form exists (Edelhoch et al., 1968), however, still exhibit multiexponential fluorescence decay. Those tyrosine derivatives with a titratable carboxyl group have fluorescence decay kinetics more complex than the simple two-state, ground-state process seen with PPA. In these cases another ground-state mechanism, or mechanisms, must be important besides the number of chemical species.

Gauduchon & Wahl (1978) proposed that the complex fluorescence decay of tyrosylglycine at pH 5.5 was the result

of rotamer populations persisting on the nanosecond time scale. This hypothesis states that each rotamer has a different environment, thus creating the required microheterogeneity; the different chemical environments cause each rotamer to have its own characteristic decay rate. If the rotamer interconversion is fast compared to the depopulation of the individual rotamer excited states, then an average emitting species results with one apparent lifetime. If the rotamer interconversion is slow, then the amplitude of the decay of each rotamer should reflect the ground-state rotamer populations. Data analysis should resolve these amplitudes, provided the three rotamers have sufficiently different lifetimes with significant fractional intensities. If the interconversion is on the same time scale as the decay of the excited states, then the system is undergoing excited-state reactions. The initial excited-state populations will be determined by the equilibrium ground-state populations, but the excited-state populations, and therefore the observed fluorescence decay amplitudes, will be determined by the rates of rotamer exchange and, hence, will not reflect the ground-state populations. In addition, the measured fluorescence lifetimes of the individual rotamers will not be their intrinsic fluorescence lifetimes but will be influenced by the rotamer exchange rates.

On the basis of the above considerations and the limitations of the rotamer model, observation of multiexponential decays means that rotamer exchange is not fast compared to the depopulation kinetics of the phenol group in tyrosine analogues. By comparing the ground-state populations with the fluorescence decay amplitudes, it is possible to differentiate between exchange that occurs concurrent with and that occurring slower than the fluorescence time scale. Ground-state rotamer populations can be estimated from data obtained in ^{1}H NMR studies (Pople, 1958; Pachler, 1963). For this reason, we measured the ^{1}H NMR coupling constants between vicinally located C^α and C^β protons of tyrosine and its α-amino- and α-carboxyl-substituted analogues. We verified that the sample concentrations required for the NMR measurements did not affect either the fluorescence lifetimes or their relative amplitudes. Fluorescence decay measurements at high and low concentrations in D_2O, the solvent used in the NMR experiments, gave identical results. Although the isotope effect in D_2O increases the lifetimes relative to those in H_2O, the relative amplitudes are unaffected.

The ^{1}H NMR results in Table III show that all three phenol rotamers have finite populations in the compounds studied. Thus, for the tyrosine compounds without a titratable carboxyl group, on the basis of the rotamer model, we expect three fluorescence lifetimes between 0 and approximately 3 ns, provided that interconversion between rotamers is slow. Resolution of three decay times within these short time limits is difficult, particularly if two or three of them are similar. The relevant compounds without a carboxyl group are tyrosinamide and *N*-acetyltyrosinamide and, in a limited way, the zwitterion form of tyrosylglycine. These compounds are adequately fit by two exponentials, one that is subnanosecond and another that is near 2 ns (Table II). The amplitude of the shorter decay time for tyrosinamide is similar to the ^{1}H NMR determined rotamer II population, whereas the corresponding amplitude for tyrosylglycine could be associated with either rotamer I or II, and the shorter component amplitude for *N*-acetyltyrosinamide is closest to rotamer III. If these correlations are not fortuitous, the fluorescence data suggest either that two of the rotamers have similar decay kinetics or that exchange is rapid between those two rotamers, averaging their excited-state behavior. Also, there is no obvious way to assign the shorter decay time to a particular rotamer.

Table IV: Fluorescence Decay Parameters Based on a Rotamer/Linked-Amplitude Analysis

compd	α_1[a]	τ_1 (ns)	α_2[a]	τ_2 (ns)	α_3[a]	τ_3 (ns)
tyrosinamide[b]	0.46	2.0	0.37	0.39	0.17	1.55
tyrosinamide[b]	0.46	1.78	0.37	0.38	0.17	2.21
N-acetyltyrosinamide	0.60	2.33	0.32	1.73	0.08	0.54
tyrosylglycine[c]	0.43	2.55	0.38	0.71	0.19	1.91
tyrosylglycine[c,d]	0.55	2.46	0.30	0.63	0.15	1.25

[a] Amplitudes were normalized to a sum of 1.0. [b] Final lifetimes were very sensitive to the value of an initial guess and its association with a particular amplitude. [c] In its zwitterionic form. [d] A free-floating analysis for all parameters (no amplitude linkage).

The rotamer model can be tested by a null hypothesis: the data can be analyzed for three components, linking the amplitudes to the NMR-determined rotamer populations. If the rotamer model fails in the slow-exchange limit, worse statistical parameters would be expected for the data fits; if the fits are as good as or better than the two-component, free-floating analysis, then the rotamer model remains viable. Table IV summarizes the results of these single-curve, linked-function analyses (Ross et al., 1986b). In each case, the statistical parameters describing the fits were as good as or better than those obtained for a two-component, free-floating analysis. According to the amplitude linkage, rotamer II can be assigned to the shortest lifetime of tyrosinamide; the other two rotamer lifetimes are similar. This analysis was sensitive to correlation of amplitude with initial lifetime values. Nevertheless, *the only statistically satisfactory analysis correlated the shortest lifetime with rotamer II.* The same result, but with less sensitivity to the lifetime guesses, is obtained for tyrosylglycine. In the case of tyrosylglycine, rotamers I and II have nearly identical populations, and it is not surprising that the free-floating analysis fails to distinguish them. It should be noted that a free-floating, three-component analysis for tyrosylglycine (without linking the amplitudes to the ground-state rotamer populations) yielded results not only close to those obtained with the linked analysis but also with slightly improved statistics compared with the two-component, free-floating fit. The linked-amplitude analysis results for *N*-acetyltyrosinamide also show two similar lifetimes for two rotamers. But in contrast to the previous two compounds, the shortest decay time associates with rotamer III. In all three cases it might be argued that several combinations of three components could provide a better fit than two. But statistically adequate fits with linked amplitudes were obtained only with the associations of lifetimes and amplitudes described above.

Introduction of a titratable α-carboxyl group complicates the fluorescence decay kinetics: the number of ground-state chemical species, and therefore possible emitting species, increases by a factor of 2. For the rotamer model in the slow-exchange limit there will be six possible emitters when the pH is in the neighborhood of the α-carboxyl pK_a. Tyrosine, *O*-methyltyrosine, *N*-acetyltyrosine, and glycyltyrosine are in this category. When the α-carboxyl group of tyrosine or *O*-methyltyrosine is fully ionized, the fluorescence decay data can be fit by a single exponential, although the statistical criteria do not indicate that the fit is truly satisfactory. Attempts to add a second component in a free-floating analysis fail. When substitution is made at the α-amino group, a single exponential decay law is clearly inadequate, but again attempts to add a second component fail. According to the rotamer model, this behavior could be due either to rotamers with very similar lifetimes or to rotamer exchange occurring on the time scale of the fluorescence decay.

Detailed analysis of the protonated carboxyl form of tyrosine compounds was carried out on *N*-acetyltyrosine since it has the highest pK_a of the compounds studied [about 3.7 (Edelhoch et al., 1968)]. This allows study of the fully protonated form without interference caused by dynamic quenching from high concentrations of H^+. A satisfactory free-floating analysis of the fully protonated form requires at least two exponentials. Both lifetimes are shorter than the "single" lifetime obtained for the fully ionized species, and the relative quantum yields calculated from the lifetimes of the fully protonated and fully ionized species agree with the steady-state titration data of Edelhoch et al. (1968). The amplitude associated with the shorter lifetime of the fully protonated species corresponds with the rotamer II population, as was found for tyrosinamide and tyrosylglycine.

The low-pH fluorescence decay data of *N*-acetyltyrosine is consistent with the slow-exchange rotamer model. Figure 3, as explained under Results, demonstrates that the pH dependence of *N*-acetyltyrosine decay kinetics is more complex than the two-state, ground-state behavior of PPA. But, since the steady-state fluorescence titration data follow simple two-state, ground-state behavior, as predicted by the Henderson–Hasselbalch relationship, we expect that the time-resolved fluorescence parameters should also reflect this relationship. If the data are not being analyzed by the correct model, the possibility of rotamer populations with different decay times for both the protonated and deprotonated forms might result in an unrecognizable pattern for the decay parameters as a function of pH; yet adequate fitting statistics might be obtained. Clearly, a two-component, free-floating analysis is not going to account for the complex decay law required by rotamers superimposed on the two-state, ground-state titration. As previously stated, the expected model requires six possible decay constants. These decay constants should be pH-independent, and the combined amplitudes for the protonated and deprotonated species will exhibit a Henderson–Hasselbalch linkage. Furthermore, the three amplitudes associated with either chemical species should also be linked by the ^{1}H NMR determined rotamer populations.

To resolve six decay constants, we attempted to overdetermine the data base by analyzing the entire pH data set using the global approach (Knutson et al., 1983; Beechem et al., 1983). The global model applied to these data assumed pH-independent lifetimes common to all decay curves. At the first level of sophistication, the data were analyzed for three components on the basis of the results of the free-floating analyses of the fully protonated (two components) and fully ionized (one component) α-carboxyl of *N*-acetyltyrosine. The results of this analysis are shown in Figure 5A. All statistical parameters describing the quality of the fits were as good as obtained by the previous curve-by-curve analyses. On the basis of this three-component model, the fully ionized carboxyl species exhibits a single lifetime while the fully protonated form displays two exponentials. It is interesting to note that as a function of pH the amplitude associated with the shorter lifetime of the protonated species is a constant fraction of the sum total of the amplitudes for that species. Moreover, that fraction correlates with the population found for rotamer II. The summed amplitudes of the protonated species and the amplitude of the ionized component follow the expected titration behavior. It must be emphasized that the global fitting assumed nothing about either the pH-dependent behavior of the amplitudes or the rotamer populations. Therefore, the three-component global fit successfully extracts the two-state,

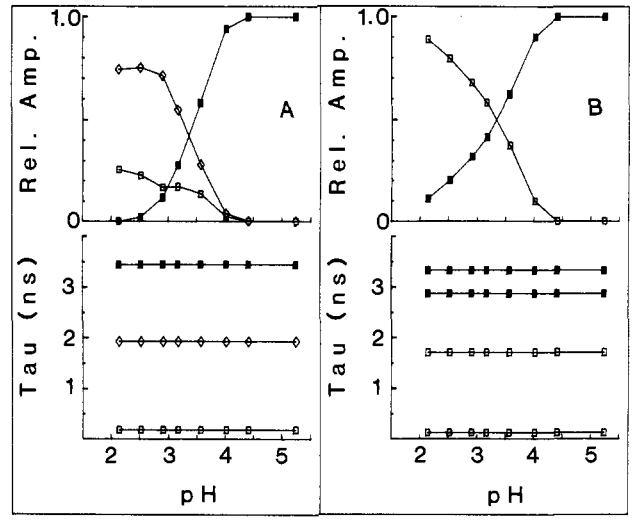

FIGURE 5: Global analysis of the *N*-acetyltyrosine fluorescence decay data set shown in Figure 3. (Panel A) A three-component analysis assuming three common lifetimes over the pH range. (Panel B) A four-component analysis assuming four common lifetimes. Symbol associations relate each lifetime with its amplitude, except in panel B where the relative amplitudes displayed are the sum of the preexponentials of the two symbol-associated lifetimes. Solid lines join related data points.

ground-state α-carboxyl titration, while still supporting the slow-exchange rotamer hypothesis in the case of fully protonated *N*-acetyltyrosine.

A possible explanation for the poor single exponential fit of fully ionized *N*-acetyltyrosine is rotamers with similar lifetimes. We considered that a global fit for four components (out of the possible six), as the next level of analysis sophistication, could yield two decay times associated with each chemical species. An alternate possibility is that the protonated species could exhibit three components while the ionized species exhibits one. The initial results of global analysis with four common lifetimes showed, however, an unrecognizable pattern for the amplitudes as a function of pH, even though the lifetime associated with the ionized carboxyl form appeared to split into two components with similar time constants. Various combinations of the sum of two amplitudes compared against the sum of the other two indicated only one physically reasonable pairing: the two longer lifetimes associated with the ionized species and the two shorter lifetimes associated with the protonated form. When this association is made, the sum of the amplitudes of each species follows the Henderson–Hasselbalch relation as shown in Figure 5B. Considering the difficulties involved in obtaining a reasonable four-component global analysis, we could not justify further analysis including additional components. Work is currently under way to develop a global approach utilizing linked functions in concert with common parameters that have a known pH dependence (Ross et al., 1968b). This will permit analysis of the entire pH data set for compliance with the combined rotamer and α-carboxyl titration, six-component model.

Previous work by Tournon et al. (1972) suggested that the carbonyl group could quench aromatics efficiently by a charge-transfer mechanism. A direct interaction between the carbonyl group and the phenol ring, resulting in quenching of the excited state, was previously suggested by Cowgill (1963a,b, 1967) and Feitelson (1969). It is also reasonable that quenching is more efficient with protonated carboxyl groups since ionization would diminish the electron-accepting capability of the carbonyl function. It can be seen in Figure 4 that the phenol ring is in close proximity to the carbonyl

group in rotamers II and III. Consistent with this observation, in no case was rotamer I associated with the shortest decay time. Indeed, in all but one case, the shortest lifetime can be associated with rotamer II. As will be discussed in the following paper (Ross et al., 1986a), fluorescence decay data for small polypeptides containing a single tyrosyl residue also indicate rotamer II as having the shortest lifetime.

Implicit in the above analyses is the assumption that the molar extinction coefficient of the phenol ring is essentially the same in all three rotamers. This is a reasonable assumption since the chemical perturbation produced by the different rotamer environments will be dominated by the hydrogen bonding of the phenol ring hydroxyl group to water, as well as by the dipolar interaction with water. Thus, change of only a few percent would be expected in the tyrosyl absorption of any one rotamer compared with that of another [Wetlaufer (1962)]. In this case, within the error of measurement, the fluorescence quantum yields reflect the excited-state depopulation kinetics of the individual rotamers.

We clearly recognize that kinetics cannot prove a given model; models can only be rejected. With this caveat in mind, we summarize our results as follows: first, the multiexponential fluorescence decay kinetics observed with tyrosine derivatives with a blocked or protonated α-carboxyl group fit a rotamer model in which at least one rotamer is slow to exchange on the nanosecond time scale with the other two rotamers and are consistent with all three rotamers interconverting slowly; second, tyrosine and its derivatives with an ionizable α-carboxyl group exhibit complex decay kinetics as a function of pH that can be resolved in terms of the rotamer model superimposed on the titration curve of the carboxyl group; third, in several cases a correlation can be made between the shortest decay constant and rotamer II; fourth, the single exponential fit for the decay of the tyrosine zwitterion is consistent with the rotamers either having similar lifetimes or interconverting rapidly; and fifth, protonation of the α-carboxyl group appears either to quench the excited-state rotamers differentially or to slow rotamer interconversion.

ACKNOWLEDGMENTS

We thank Dr. Satish Joshi for the thin-layer chromatography analyses, Dr. Jack Preses for assistance with program conversion to the VAX, and Dr. Panayotis G. Katsoyannis for his continued interest. We also thank Drs. August Maki, Robert Dale, and Lesley Davenport for helpful and critical discussions.

Registry No. PPA, 501-97-3; phenol, 108-95-2; anisole, 100-66-3; *p*-cresol, 106-44-5; tyramine, 51-67-2; tyrosine, 60-18-4; *O*-methyltyrosine, 6230-11-1; *N*-acetyltyrosine, 537-55-3; glycyltyrosine, 658-79-7; tyrosinamide, 4985-46-0; *N*-acetyltyrosinamide, 1948-71-6; tyrosylglycine, 673-08-5.

REFERENCES

Azumi, T., & McGlynn, S. P. (1962) *J. Chem. Phys. 37*, 2413–2420.

Badea, M. G., & Brand, L. (1979) *Methods Enzymol. 61*, 378–425.

Beechem, J. M., Knutson, J. R., Ross, J. B. A., Turner, B. W., & Brand, L. (1983) *Biochemistry 22*, 6054–6058.

Chang, M. C., Petrich, J. W., McDonald, D. B., & Fleming, G. R. (1983) *J. Am. Chem. Soc. 105*, 3819–3824.

Cornog, J. L., & Adams, W. R. (1963) *Biochim. Biophys. Acta 66*, 356–365.

Cowgill, R. W. (1963a) *Arch. Biochem. Biophys. 100*, 36–44.

Cowgill, R. W. (1963b) *Biochim. Biophys. Acta 75*, 272–273.

Cowgill, R. W. (1967) *Biochim. Biophys. Acta 133*, 6–18.

Creed, D. (1984) *Photochem. Photobiol. 39*, 563–575.

Donzel, B., Gauduchon, P., & Wahl, Ph. (1974) *J. Am. Chem. Soc. 96*, 801–808.

Edelhoch, H., Perlman, R. L., & Wilchek, M. (1968) *Biochemistry 7*, 3893–3900.

Feitelson, J. (1964) *J. Phys. Chem. 68*, 391–397.

Feitelson, J. (1969) *Photochem. Photobiol. 9*, 401–410.

Fischman, A. J., Wyssbrod, H. R., Agosta, W. C., & Cowburn, D. (1978) *J. Am. Chem. Soc. 100*, 54–58.

Gafni, A., & Brand, L. (1978) *Chem. Phys. Lett. 58*, 346–350.

Gafni, A., Modlin, R. L., & Brand, L. (1976) *J. Phys. Chem. 80*, 898–904.

Gauduchon, P., & Wahl, Ph. (1978) *Biophys. Chem. 8*, 87–104.

Greenstein, J. P., & Winitz, M. (1961) in *Chemistry of the Amino Acids*, p 498, Wiley, New York.

Grinvald, A., & Steinberg, I. Z. (1974) *Anal. Biochem. 59*, 583–598.

Kalantar, A. H. (1968) *J. Chem. Phys. 48*, 4992–4996.

Kendrew, J. C., Klyne, W., Lifson, S., Miyazawa, T., Nēmethy, G., Phillips, D. C., Ramachandran, G. N., & Scheraga, H. A. (1970) *Biochemistry 9*, 3471–3479.

Kirby, G. W., & Michael, J. (1971) *J. Chem. Soc., Chem. Commun.*, 187–188.

Knight, A. E. W., & Selinger, B. K. (1971) *Chem. Phys. Lett. 10*, 43–48.

Knutson, J. R., Beechem, J. M., & Brand, L. (1983) *Chem. Phys. Lett. 102*, 501–507.

Laws, W. R., & Brand, L. (1979) *J. Phys. Chem. 83*, 795–802.

Laws, W. R., & Sutherland, J. C. (1986) *Photochem. Photobiol.* (in press).

Laws, W. R., Sutherland, J. C., Ross, J. B. A., Chanley, J. D., Katsoyannis, P. G., Buku, A., & Wyssbrod, H. R. (1984) *Photochem. Photobiol. 39S*, 94S (Abstr. THPM-B4).

Laws, W. R., Ross, J. B. A., Sutherland, J. C., Katsoyannis, P. G., Buku, A., & Wyssbrod, H. R. (1985) *Biophys. J. 47*, 411a (Abstr. W-Pos72).

Longworth, J. W. (1971) in *Excited States of Proteins and Nucleic Acids* (Steiner, R. F., & Weinryb, I., Eds.) pp 319–484, Plenum Press, New York.

Longworth, J. W. (1981) *Ann. N.Y. Acad. Sci. 366*, 237–245.

Longworth, J. W. (1983) in *Time-Resolved Fluorescence Spectroscopy in Biochemistry and Biology* (Cundall, R. B., & Dale, R. E., Eds.) pp 651–725, Plenum Press, New York.

Longworth, J. W., & Rahn, R. O. (1967) *Biochim. Biophys. Acta 147*, 526–535.

Pachler, K. G. R. (1963) *Spectrochim. Acta 19*, 2085–2092.

Pachler, K. G. R. (1964) *Spectrochim. Acta 20*, 581–587.

Paoletti, J., & LePecq, J.-B. (1969) *Anal. Biochem. 31*, 33–41.

Petrich, J. W., Chang, M. C., McDonald, D. B., & Fleming, G. R. (1983) *J. Am. Chem. Soc. 105*, 3824–3832.

Pople, J. A. (1958) *Mol. Phys. 1*, 3–8.

Rayner, D. M., Krajcarski, D. T., & Szabo, A. G. (1978) *Can. J. Chem. 56*, 1238–1245.

Robbins, R. J., Fleming, G. R., Beddard, G. S., Robinson, G. W., Thistlethwaite, P. J., & Woolfe, G. J. (1980) *J. Am. Chem. Soc. 102*, 6271–6279.

Ross, J. B. A., Rousslang, K. W., & Brand, L. (1981) *Biochemistry 20*, 4361–4369.

Ross, J. B. A., Laws, W. R., Buku, A., Sutherland, J. C., & Wyssbrod, H. R. (1986a) *Biochemistry* (following paper in this issue).

Ross, J. B. A., Laws, W. R., Sutherland, J. C., Buku, A., Katsoyannis, P. G., Schwartz, I. L., & Wyssbrod, H. R. (1986b) *Photochem. Photobiol.* (in press).

Shinitzky, M. (1972) *J. Chem. Phys. 56*, 5979–5981.
Szabo, A. G., & Rayner, D. M. (1980) *J. Am. Chem. Soc. 102*, 554–563.
Tournon, J., Kuntz, E., & El Bayoumi, M. A. (1972) *Photochem. Photobiol. 16*, 425–433.
Weller, A. (1961) *Prog. React. Kinet. 1*, 189–214.
Wetlaufer, D. B. (1962) *Adv. Protein Chem. 17*, 303–390.
White, A. (1959) *Biochem. J. 71*, 217–220.
Wyssbrod, H. R., Ballardin, A., Schwartz, I. L., Walter, R., Van Binst, G., Gibbons, W. A., Agosta, W. C., Field, F. H., & Cowburn, D. (1977) *J. Am. Chem. Soc. 99*, 5273–5276.

Time-Resolved Fluorescence and ^{1}H NMR Studies of Tyrosyl Residues in Oxytocin and Small Peptides: Correlation of NMR-Determined Conformations of Tyrosyl Residues and Fluorescence Decay Kinetics†

J. B. Alexander Ross,*,‡ William R. Laws,*,§,‖ Angeliki Buku,⊥ John Clark Sutherland,§ and Herman R. Wyssbrod*,⊥,#

Department of Biochemistry, Department of Physiology and Biophysics, and Center for Polypeptide and Membrane Research, Mount Sinai School of Medicine, New York, New York 10029, and Biology Department, Brookhaven National Laboratory, Upton, New York 11973

Received June 27, 1985

ABSTRACT: Steady-state and time-resolved fluorescence properties of the single tyrosyl residue in oxytocin and two oxytocin derivatives at pH 3 are presented. The decay kinetics of the tyrosyl residue are complex for each compound. By use of a linked-function analysis, the fluorescence kinetics can be explained by a ground-state rotamer model. The linked function assumes that the preexponential weighting factors (amplitudes) of the fluorescence decay constants have the same relative relationship as the ^{1}H NMR determined phenol side-chain rotamer populations. According to this model, the static quenching of the oxytocin fluorescence can be attributed to an interaction between one specific rotamer population of the tyrosine ring and the internal disulfide bridge.

Steady-state fluorescence studies of peptides and polypeptides in aqueous solution have used all three aromatic amino acids, phenylalanine, tyrosine, and tryptophan, as intrinsic probes [see reviews by Schiller (1981), Longworth (1983), and Creed (1984a,b)]. By contrast, time-resolved fluorescence investigations have emphasized the use of tryptophan (Beechem & Brand, 1985). Less has been done with tyrosine, and phenylalanine has been virtually ignored, since both amino acids have considerably weaker absorption than tryptophan and small quantum yields when incorporated into peptides and proteins (Longworth, 1971). Furthermore, in those molecules containing both tyrosine and tryptophan, tryptophan emission strongly masks tyrosine emission, although the fluorescence of tyrosine has been resolved in careful steady-state (Eisinger, 1969; Eisinger et al., 1969) and time-resolved (Brochon et al., 1974; Lakowicz & Cherek, 1981) studies.

We are interested in how the time-resolved fluorescence kinetics of the aromatic amino acids, especially tryptophan and tyrosine, may be used to obtain information about peptide conformations in dilute solution. As recently reviewed by Beechem & Brand (1985), the fluorescence decay kinetics of most single-tryptophan-containing peptides are complex. The mechanism for the observed kinetics of tryptophan and tryptophyl-containing peptides is not clear. Several possibilities have been mentioned in the literature, including indole photochemistry involving exchange of the C-4 indole hydrogen (Saito et al., 1984) and environmental effects resulting from the three principle different rotameric conformers of the indole side chain (Szabo & Rayner, 1980; Robbins et al., 1980; Ross et al., 1981; Chang et al., 1983; Petrich et al., 1983).

It has recently been found by Libertini & Small (1985) that the single tyrosine residue in histone H1 exhibits complex fluorescence decay kinetics. As shown in the preceding paper in this issue (Laws et al., 1986), the fluorescence decay kinetics of simple tyrosine analogues are also complex. Direct comparison of the ^{1}H NMR[1] determined rotamer populations with the fluorescence data, however, indicates that the complex kinetics seen for tyrosine compounds are readily explained in terms of a rotamer model. In the rotamer model, three chemically distinct environments exist for the phenol ring about the C^α–C^β bond.

In the present paper, we extend the results of the preceding paper (Laws et al., 1986) by examining the fluorescence decay kinetics of a single tyrosyl residue in small, cyclic peptides.

† Supported by NIH Grants HD-17542 (J.B.A.R.) and AM-10080 (H.R.W.) and in part by NIH Grant AM-12925 and the Life Sciences Foundation, Inc. A.B. is supported by NIH Grant AM-10080. W.R.L., J.C.S., and the fluorescence spectrometer at station U9B of the National Synchrotron Light Source (NSLS) are supported by the Office of Health and Environmental Research, U.S. Department of Energy (USDOE). The NSLS is supported by the Office of Energy Research, USDOE. During part of this project, W.R.L. was supported by NIH Training Grant CA-09121. The NMR spectroscopy laboratory at Hunter College is supported by NSF Grant PGM-111745. Preliminary aspects of this work were presented at the 29th Annual Meeting of the Biophysical Society held in Baltimore, MD, Feb 1985 (Laws et al., 1985).

* Authors to whom correspondence should be addressed.
‡ Department of Biochemistry, Mount Sinai School of Medicine.
§ Brookhaven National Laboratory.
‖ Present address: Center for Polypeptide and Membrane Research, Mount Sinai School of Medicine, New York, NY 10029.
⊥ Center for Polypeptide and Membrane Research, Mount Sinai School of Medicine.
Department of Physiology and Biophysics, Mount Sinai School of Medicine.

[1] Abbreviation: ^{1}H NMR, proton nuclear magnetic resonance.

0006-2960/86/0425-0607$01.50/0